Original Article

The landscape of m6A regulators in esophageal cancer: molecular characteristics, immuno-oncology features, and clinical relevance

Zhe Li[1], Chunyan Zheng[1], Liquan Huang[2], Xiaoyang Yin[1], Zhongtang Wang[1], Chengxin Liu[1], Baosheng Li[1]

[1]Department of Radiation Oncology, Shandong Cancer Hospital and Institute, Shandong First Medical University and Shandong Academy of Medical Sciences, Jinan, China; [2]Department of Anesthesiology, Shandong Cancer Hospital and Institute, Shandong First Medical University and Shandong Academy of Medical Sciences, Jinan, China

Contributions: (I) Conception and design: Z Li, B Li; (II) Administrative support: Z Wang, B Li; (III) Provision of study materials or patients: C Zheng, L Huang; (IV) Collection and assembly of data: Z Li, C Liu; (V) Data analysis and interpretation: Z Li, X Yin; (VI) Manuscript writing: All authors; (VII) Final approval of manuscript: All authors.

Correspondence to: Baosheng Li. Department of Radiation Oncology, Shandong Cancer Hospital and Institute, Shandong First Medical University and Shandong Academy of Medical Sciences, No. 440, Jiyan Road, Jinan, China. Email: bsli@sdfmu.edu.cn.

Background: Squamous cell carcinoma (SCC) and adenocarcinoma (AC) are the two main pathological types of esophageal cancer (EC), which differ in molecular features, genetic variation, and treatment sensitivity. However, as a key process in tumorigenesis and development, the role of N6-methyladenosine (m6A) regulators in esophageal squamous cell carcinoma (ESCC) and esophageal adenocarcinoma (EAC) is not fully understood.

Methods: This study systematically compared the role of m6A regulators of ESCC and EAC in terms of molecular characteristics, immuno-oncology characteristics, and clinical relevance, and validated our findings in a long-term follow-up patient cohort.

Results: There were many differences in m6A regulators between ESCC and EAC in terms of expression patterns, genetic variation, association with tumor pathways, immune signatures, and immunotherapy sensitivity. Furthermore, *VIRMA* was identified as a factor with opposite functional and prognostic effects in ESCC and EAC. ESCC patients with high *VIRMA* expression and EAC patients with low *VIRMA* expression had a better prognosis. Single-center data showed that low expression of *FTO* may be associated with superior immunotherapy efficacy in ESCC patients.

Conclusions: The results herein provide novel ideas for understanding the tumor characteristics, occurrence, and development of ESCC and EAC, and suggest new targets for the treatment and intervention of EC.

Keywords: N6-methyladenosine (m6A); esophageal squamous cell carcinoma (ESCC); esophageal adenocarcinoma (EAC); tumor characteristics; immunotherapy

Submitted Nov 14, 2022. Accepted for publication Dec 13, 2022.
doi: 10.21037/atm-22-5895
View this article at: https://dx.doi.org/10.21037/atm-22-5895

Introduction

Esophageal cancer (EC) is a malignant tumor with the eighth highest incidence and sixth highest mortality rate in the world (1). Despite medical advances in recent years, the five-year survival rate of EC remains at 13–21% (2). As an emerging treatment modality, patients with EC have benefited from immune checkpoint inhibitors. However, based on the available data, there is a great inter-patient heterogeneity (3). Squamous cell carcinoma (SCC) and adenocarcinoma (AC) are the two main pathological types of EC. These two distinct pathological subtypes differ greatly in epidemiological characteristics, pathogenesis, and the tumor microenvironment (4,5). Therefore, understanding the mechanisms by which esophageal squamous cell

carcinoma (ESCC) and esophageal adenocarcinoma (EAC) occur and develop will contribute to the identification of intervention targets for the treatment of patients with EC.

N6-methyladenosine (m6A) is the most abundant and well-characterized internal modification of messenger RNAs (mRNAs) (6). Three types of regulators, "writers" (methyltransferases), "erasers" (demethylases), and "readers" (RNA-binding proteins), regulate the m6A process (7). A study has shown that m6A plays an important role in the occurrence, development, treatment sensitivity, and prognosis of tumors (8). However, to date, study on EC and m6a have mostly analyzed SCC and AC as a whole, which limits the usability of these study.

This current study analyzed the correlation between m6A regulators and the molecular, clinical, and immune characteristics of ESCC and EAC to provide a basis for identifying novel therapeutic interventional targets. To our knowledge, this is the first study to provide comprehensive data on the differences between ESCC and EAC in terms of m6A regulators. We present the following article in accordance with the ARRIVE reporting checklist (available at https://atm.amegroups.com/article/view/10.21037/atm-22-5895/rc).

Highlight box

Key findings

- There were many differences in m6A regulators between ESCC and EAC in terms of expression patterns, association with tumor pathways, immune signatures, and immunotherapy sensitivity. VIRMA was identified as a factor with opposite functional and prognostic effects in ESCC and EAC. Low expression of FTO may be associated with superior immunotherapy efficacy in ESCC patients.

What is known and what is new?

- M6A plays an important role in the occurrence, development, treatment sensitivity of tumors.
- We provide comprehensive data on the differences between ESCC and EAC from the perspective of m6A regulators.

What is the implication, and what should change now?

- The results herein provide novel ideas for understanding the tumor characteristics, occurrence, and development of ESCC and EAC, and suggest new targets for the treatment and intervention of EC.

Methods

Analysis of the Gene Expression Omnibus (GEO) and The Cancer Genome Atlas (TCGA) data

A total of 358 samples of the ESCC dataset GSE53625 were obtained from the GEO database, including 179 cancer and 179 normal samples. A total of 168 EC samples were obtained from TCGA (https://portal.gdc.cancer.gov/), including 78 EAC, 80 ESCC, and 10 normal control samples. TCGA data were converted to TPM regularized data, $\log_2(x+1)$ processed, and then integrated with the regularized and logarithmic GEO chip data. The batch effect was removed using the ComBat function in R package SVA. The EAC immunotherapy dataset (GSE165252) was obtained from the GEO database.

Selection of m6A regulatory factors

A total of 31 m6A regulators were selected from the literature (6-9), including 11 writers (*METTL3*, *METTL14*, *METTL16*, *METTL5*, *WTAP*, *VIRMA*, *RBM15*, *RBM15B*, *ZC3H13*, *CBLL1*, and *ZCCHC4*), 3 erasers (*FTO*, *ALKBH3*, and *ALKBH5*), and 17 readers (*YTHDF1*, *YTHDF2*, *YTHDF3*, *YTHDC1*, *YTHDC2*, *HNRNPA2B1*, *HNRNPC*, *FMR1*, *EIF3A*, *IGF2BP1*, *IGF2BP2*, *IGF2BP3*, *ELAVL1*, *G3BP1*, *G3BP2*, *PRRC2A*, and *RBMX*).

Acquisition of methylation levels, mutation sites, and copy number variation (CNV) data

The methylation level data of TCGA-ESCA and the maf file of masked somatic mutations of the ESCA cohort were obtained from TCGA, and the maf file was processed using the R package maftools. The CNV data of 176 EC samples (82 EAC and 94 ESCC) were obtained from TCGA-ESCA. We referred to the TCGA Copy Number Variation Analysis Pipeline (https://docs.gdc.cancer.gov/Data/Bioinformatics_Pipelines/CNV_Pipeline/) standards, using the following cutoff that divides the CNVs into three types, namely, gain, loss, and neutral with CNV.ratio >0.3, −0.3< CNV.ratio <0.3, and CNV.ratio <−0.3, respectively.

Table 1 Sequences of siRNA

Primer names	Sequences
VIRMA siRNA-1 sense	5'-GAGGATGATCGACGAACAGTA-3'
VIRMA siRNA-2 sense	5'-AAGGCTTATTAACCTCCTAGA-3'

Correlation analysis of immune checkpoint proteins

Sixty immune checkpoint protein-coding genes were selected, and a correlation analysis was performed using the cor() function in R, according to their expression profiles. The correlation heatmap was drawn using the R package ggcorrplot. Tumor purity, stromal score, and immune score analyses were performed using the R package ESTIMATE, and estimates of the proportion of immune cells infiltrating EC expression profiles were calculated using the R package MCP-counter.

Gene set variation analysis (GSVA) and construction of the correlation network map

Enrichment analysis of 50 cancer pathways was performed using the R package GSVA, and the correlation with the expression of m6A regulators in EC was calculated. Correlation network diagrams were drawn using Cytoscape software. A gene set of 50 hallmarks was obtained from the Msigdb database (http://www.gsea-msigdb.org/).

Clinical validation cohort

The study was conducted in accordance with the Declaration of Helsinki (as revised in 2013). The use of the validation cohort in this study was approved by the Ethics Committee of Shandong Cancer Hospital (approval No. SDTHEC201803). Since the validation cohort was retrospective in nature, the requirement for informed consent was waived.

The prognostic validation cohort included 105 ESCC and 46 EAC patients who underwent radical surgery at our hospital between December 2014 and February 2017. The inclusion criteria were pathologically confirmed ESCC and EC, and radical surgery as the first course of treatment. The exclusion criteria were a history of other malignancies, neoadjuvant therapy or salvage surgery, and incomplete medical records. Clinicopathological data of the patients were collated, and the TNM classification was used to determine the tumor stage. Patients were followed-up every 3 months for the first 3 years after treatment and every 6 months thereafter. The last follow-up was in March 2022.

The efficacy validation cohort for immune checkpoint inhibitors included 40 patients with ESCC who underwent programmed death-1 (PD-1)/programmed death ligand 1 (PD-L1) immune checkpoint inhibitor and concurrent radiotherapy and surgery in our hospital from January 2019 to June 2022. The inclusion criteria were pathologically confirmed ESCC and PD-1/PD-L1 immune checkpoint inhibitor and concurrent radiotherapy followed by surgical resection. The exclusion criteria were a medical history of other malignancies, patients without surgery, and incomplete medical records. According to the patient's surgical pathology, the tumor regression grade based on the College of American Pathologists system was used to evaluate the efficacy of immunotherapy (available at http://www.cap.org).

Cell culture

The human ESCC cell line Kyse410 and the human EAC cell line OE19 were obtained from the Key Laboratory of Shandong Cancer Hospital. Cells were cultured in Dulbecco's Modified Eagle Medium (DMEM; Gibco, USA) containing 10% fetal bovine serum (Gibco, USA) and 1% penicillin/streptomycin (Thermo Fisher Scientific, USA). All cell lines were cultured at 37 ℃ in a humidified incubator with 5% CO_2.

RNA interference (RNAi) and production of lentiviral particles

Two sets of double RNAi oligos targeting human *VIRMA* mRNA were synthesized by GenePharma (Shanghai, China). The short hairpin (sh)RNA expression plasmid (psi-LVRU6GP) was constructed by GenePharma (Shanghai, China) based on the *VIRMA* small interfering (si)RNA-1 (*Table 1*).

In vitro proliferation, invasion, and migration assays

The Kyse410 and OE19 cells were seeded in 96-well plates (2,000 cells/well) and cultured for 4 days at 37 ℃ and 5% CO_2. Each day, one 96-well plate was used, and 10 μL/well of Cell Counting Kit-8 (CCK-8) (Bioss, Beijing, China) solution was added. After culturing for 2 hours, the optical density (OD) at 450 nm was measured using a microplate reader (SpectraMax, USA). The cell proliferation rate was

calculated as follows: cell proliferation rate (%) = (OD treatment group - OD blank)/(OD control group - OD blank) ×100 (10).

Transwell chambers (Falcon, USA) with 8.0 μm transparent polyethylene terephthalate membranes were placed in 24-well plates. DMEM medium (500 μL) with 10% fetal bovine serum was added to the lower chamber, and 60,000 cells were inoculated with serum-free DMEM medium in the upper chamber. After culturing for 24–48 hours at 37 ℃ and 5% CO_2, the cells were fixed with 4% paraformaldehyde and stained with 0.1% crystal violet. After cleaning the inner membrane of the upper chamber with a cotton swab, images were observed and photographed. For the invasion assay, 100 μL of 200 μg/mL Matrigel (Corning, USA) was added, and the cells were seeded after incubation at 37 ℃ for 1 hour (11). Transwell chambers required no additional treatment for the migration assays. The cell numbers were counted in 3 different areas using an inverted microscope (Zeiss, Germany).

EC xenograft model

Animal experiments were performed under a project license (No. SDTHEC201803) granted by the Ethics Committee of Shandong Cancer Hospital, in compliance with institutional guidelines for the care and use of animals. A protocol was prepared before the study without registration. All mice were housed in a specific pathogen-free facility at the Laboratory Animal Center of Shandong Cancer Hospital. Male athymic BALB/c nude mice (BEIJING HFK BIOSCIENCE, China), aged 4–6 weeks, were reared under standard pathogen-free conditions. After shRNA interference, KYSE410 and OE19 cells (3×10^6) were injected into the right back of the mice. Tumors were measured weekly using Vernier calipers, and the tumor volume was calculated as follows: length × width^2 × 0.5 (12). Mice were euthanized after approximately 4 weeks, and tumor weights were measured using an electronic scale.

Western blot assay

Cell lysates were prepared using RIPA Lysis Buffer containing protease and phosphorylase inhibitors (Beyotime Biotechnology, China), and the BCA protein assay kit (Beyotime Biotechnology, China) was used for protein quantification. Samples were electrophoresed using 12% sodium dodecyl sulfate polyacrylamide gel electrophoresis (SDS-PAGE) and transferred to 0.22 μm polyvinylidene fluoride (PVDF) membranes (Millipore, Massachusetts, USA). After incubation with the primary antibodies, the membrane was incubated with the secondary antibody. Color development was performed using an enhanced chemiluminescence (ECL) chromogenic substrate (Millipore, Massachusetts, USA). The antibodies used in this study were as follows: *VIRMA* (1:500 dilution, #88358; Cell Signaling Technology, USA), glyceraldehyde 3-phosphate dehydrogenase (*GAPDH*; 1:1,000 dilution, #5174; Cell Signaling Technology, USA), and anti-rabbit IgG horse radish peroxidase (HRP)-linked antibody (1:2,000 dilution, #7074; Cell Signaling Technology, USA).

Immunohistochemistry (IHC) staining

Biopsy pathological specimens were routinely fixed in 10% neutral buffered formalin, cut into 4 μm sections, dried at 65 ℃ for 1 hour, dewaxed with xylene, and rehydrated with graded ethanol series. Antigens were recovered by heating samples in ethylenediaminetetraacetic acid (EDTA; pH 8.0) at 95 ℃ for 15–20 minutes. Endogenous peroxidase was blocked by incubating the sections with 3% hydrogen peroxide for 15 minutes. After protein blocking for 15 minutes, the cells were mixed with primary antibodies including anti-*FTO* (1:2,000, 27226-1-AP, Proteintech, China), anti-*VIRMA* (1:1,000, 25712-1-AP, Proteintech, China), anti-*RBM15B* (1:250, 22249-1-AP, Proteintech, China), anti-*METTL14* (1:500, 26158-1-AP, Proteintech, China), and anti-*WTAP* (1:500, 60188-1-Ig, Proteintech, China) and incubated overnight at 4 ℃. Negative controls were incubated with phosphate-buffered saline (PBS) instead of a primary antibody. The next day, slides were heated at room temperature for 1 hour, washed 3 times with PBS for 5 minutes each, and then treated with the Novolink polymer for 10–15 minutes. According to the resistance, the slides were incubated with an appropriate amount of biotin-labeled goat anti-rabbit/mouse IgG polymer for 10–15 minutes at room temperature and followed by 2 washes with PBS. Slides were then incubated with horseradish-labeled streptomycin working solution for 10–15 minutes and washed 3 times with PBS. The DAB working solution (1:20 DAB chromogen in DAB substrate buffer, Novolink) was prepared and applied for 3 minutes, counterstained with hematoxylin (Novolink) for 2 min, and dehydrated. All images were obtained using a BX53 fluorescence microscope (Olympus Corporation, Tokyo, Japan).

The degree of staining was calculated as the proportion of positively stained tumor cells score (PP) multiplied by

the staining intensity score (SI) (13). The PP scoring was as follows: 0 (<5%, negative), 1 (5–25%, sporadic), 2 (26–50%, focal), and 3 (>51%, diffuse). SI scores were divided into the following 4 categories: 0, negative staining; 1, weak staining; 2, moderate staining; and 3, strong staining. Scoring was performed independently by two pathologists who were blinded to the clinical characteristics and grouping. Any disagreements were resolved via discussion. The degree of staining was classified as follows: 0–3 (low expression) and 4–9 (high expression).

Statistical analysis

Survival analysis of EC samples was performed using the R package survminer according to the patients' clinical information. The Kaplan-Meier survival curve was tested for significance using the R package ggpubr. The log-rank test was used for statistical testing of all survival curves. All statistical tests between the two groups in this study were calculated using the stat_compare_mean() function of the R package ggpubr using the Wilcoxon test method. Statistical significance was indicated by P values less than 0.05 as follows: *, P<0.05, **, P<0.01, ***, P<0.001, and ****, P<0.0001.

Results

Expression patterns and genetic variations of m6A regulators in EC

A total of 31 m6A regulators were identified from published articles (6-9,14), including 11 writers, 3 erasers, and 17 readers (Figure S1A). The expression of these regulators was assessed using the TCGA-ESCA dataset and their distribution in the genome is shown in Figure S1B. The principal component analysis showed that the expression profiles of the m6A regulators in EAC and ESCC could differentiate between the two subtypes (*Figure 1A*).

The expressions of m6A regulators in the TCGA-ESCA transcriptome data and the microarray data of GSE53625 showed that there were 13 differentially expressed regulatory factors (*ALKBH3*, *ALKBH5*, *ELAVL1*, *FTO*, *G3BP1*, *HNRNPC*, *METTL16*, *METTL3*, *METTL5*, *PRRC2A*, *WTAP*, *YTHDC1*, and *YTHDF2*) between the ESCC and ECA groups (*Figure 1B*), all of which were expressed at higher levels in ESCC. In the EAC group, the differentially expressed regulators showed higher expression in the tumor tissues compared to normal tissues (Figure S1C). In the ESCC group, the expression levels of *EIF3A*, *METTL14*, *RBM15*, *YTHDC1*, and *YTHDC2* were higher in normal tissues compared to tumor tissues (Figure S1D).

CNV frequency changes in m6A regulators were very common in the TCGA-ESCA samples, with most showing increased CNVs. CNV was lower in the two writers, *RBMX* and FMR1, in EAC and ESCC, and also in *RBM15B* in ESCC (*Figure 1C,1D*).

Regarding somatic mutations, the most mutated regulator in EAC was *ZC3H13*, followed by *PRRC2A*, *FMR1*, and *EIF3A* (*Figure 1E*). The regulators with the highest mutation rates in ESCC were *RBM15*, *ZC3H13*, and *ALKBH3* (*Figure 1F*). Mutations were observed for all three erasers in ESCC, but not in the EAC data. Combined with *Figure 1B*, it can be observed that the RNA expression these 3 regulators are higher in ESCC than in EAC. Therefore, we suggest that the occurrence of genetic variation is common in EAC, and these changes are related to the expression levels of regulatory factors.

Association of m6A regulators with tumor stage and prognosis in EC

The association between m6A regulators and the TNM stage was analyzed (Figure S2). Among patients with advanced T stage, the expression level of *FMR1* was increased in EAC patients, and the expression levels of *CBLL1*, *HNRHPA2B1*, *VIRMA*, *YTHDF3*, *ZC3H13*, and *ZCCHC4* were increased in ESCC patients. None of the m6A regulators showed any significant difference in expression between tumors with and without lymph node metastasis. In terms of M staging, EAC patients with distant metastasis had higher expression levels of *EIF3A*, *HNRHPA2B1*, *RBM15*, and *ZCCHC4*, whereas no significant differences were found in the ESCC group. Regarding clinical staging, *FMR1* and *IGF2BP3* were highly expressed in patients with advanced EAC and ESCC stages, respectively, while *YTHDF2* was highly expressed in early staging.

Survival analysis of TCGA data showed that the expressions of *G3BP1*, *HNRNPA2B1*, *METTL5*, *RBMX*, *VIRMA*, and *WATP* were negatively associated with survival in patients with EAC (*Figure 2*). In ESCC, only *VIRMA* was significantly associated with overall survival. Interestingly, *VIRMA* showed an opposite trend in ESCC compared with EAC patients, that is, patients with low *VIRMA* expression had poor prognosis.

In our retrospective validation analysis, surgical

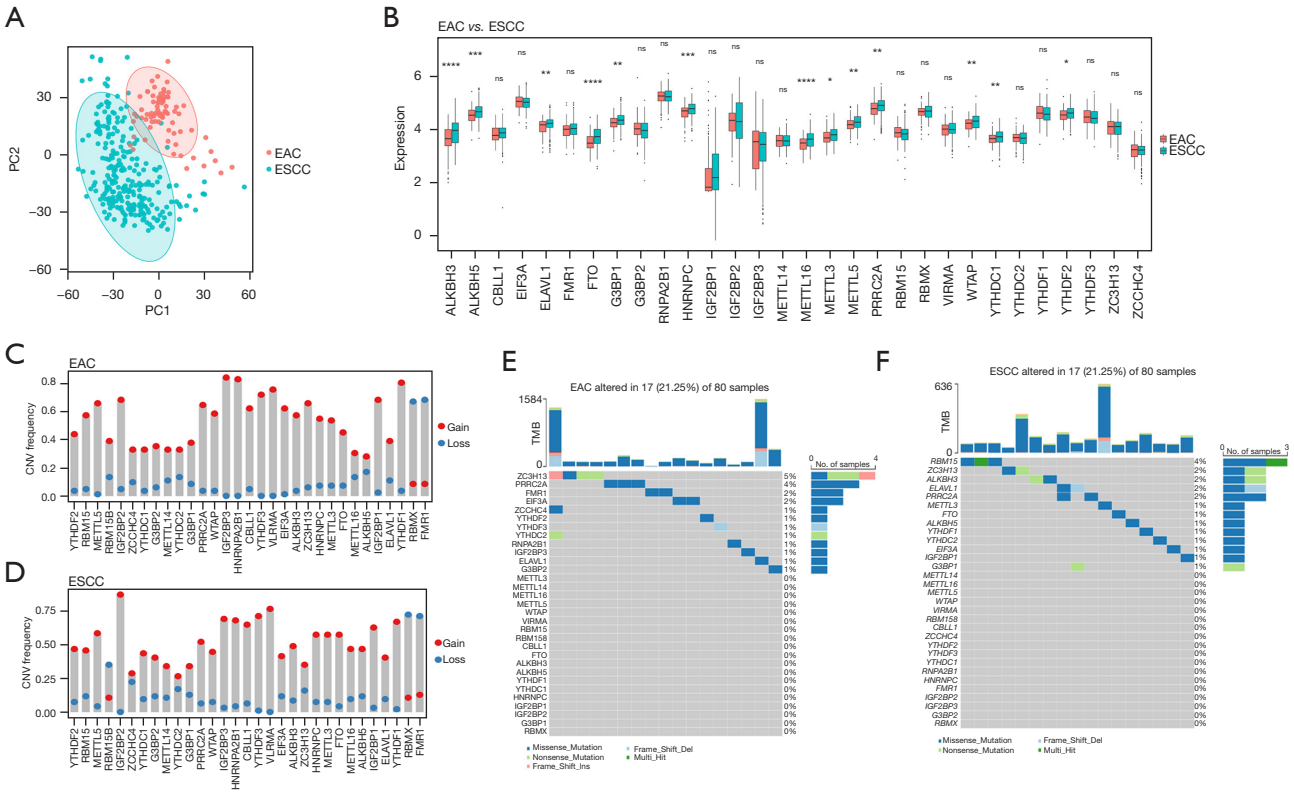

Figure 1 The expression patterns and genetic variations of m6A regulators. (A) Principal component analysis of the expression profiles of 31 m6A regulators used to differentiate SCs and ACs in the TCGA-ESCA cohort. Red represents EAC samples, and green represents ESCC samples. (B) A comparison of the expression levels between EAC and ESCC in the TCGA-ESCA and GSE53625 datasets. Red represents EAC samples, and green represents ESCC samples. (C,D) The copy number variation frequency of m6A regulators in 176 samples from the TCGA-ESCA dataset. Blue dots represent the deletion frequency; red dots represent the amplification frequency. The TMB refers to the total number of somatic mutations in each coding region of the tumor genome. (E,F) The mutation frequency of m6A regulators in EAC and ESCC samples from the TCGA-ESCC cohort. Each column corresponds to an individual case. The TMB is displayed as the upper bar plot. The right panel shows the mutation frequency and proportion of each variant type for each regulator. *, P<0.05, **, P<0.01, ***, P<0.001, ****, P<0.0001. EAC, esophageal adenocarcinoma; ESCC, esophageal squamous cell carcinoma; m6A, N6-methyladenosine; SC, squamous cell carcinoma; AC, adenocarcinoma; TCGA, The Cancer Genome Atlas; ESCA, esophageal cancer; TMB, tumor mutational burden; NS, no significant.

specimens were collected from 105 ESCC and 46 EAC patients, whose primary treatment was radical surgery. Through IHC and survival analysis (*Figure 3*), it was demonstrated that ESCC patients with low *VIRMA* expression had a poor prognosis, while EAC patients had a good prognosis.

The role of *VIRMA* in ESCC and EAC was further verified *in vitro*. The proliferation, migration, and invasion of the ESCC cell line Kyse410 were significantly enhanced after *VIRMA* knockdown, while the trend was the opposite in the EAC cell line OE19 (*Figure 4A-4D*). Furthermore, *in vivo* validation in a nude mouse xenograft tumor model showed that *VIRMA* knockdown resulted in markedly enhanced tumorigenicity of ESCC. In contrast, the tumorigenicity of EAC was significantly reduced (*Figure 4E*).

Association between m6A regulators and cancer pathways and immune characteristics in EC

The above analyses revealed that m6A regulators are closely related to the stage and prognosis of EC. Therefore, the role of m6A regulators in the development of EC was investigated. The correlation between m6A regulator expression and 50 cancer hallmark enrichment scores was

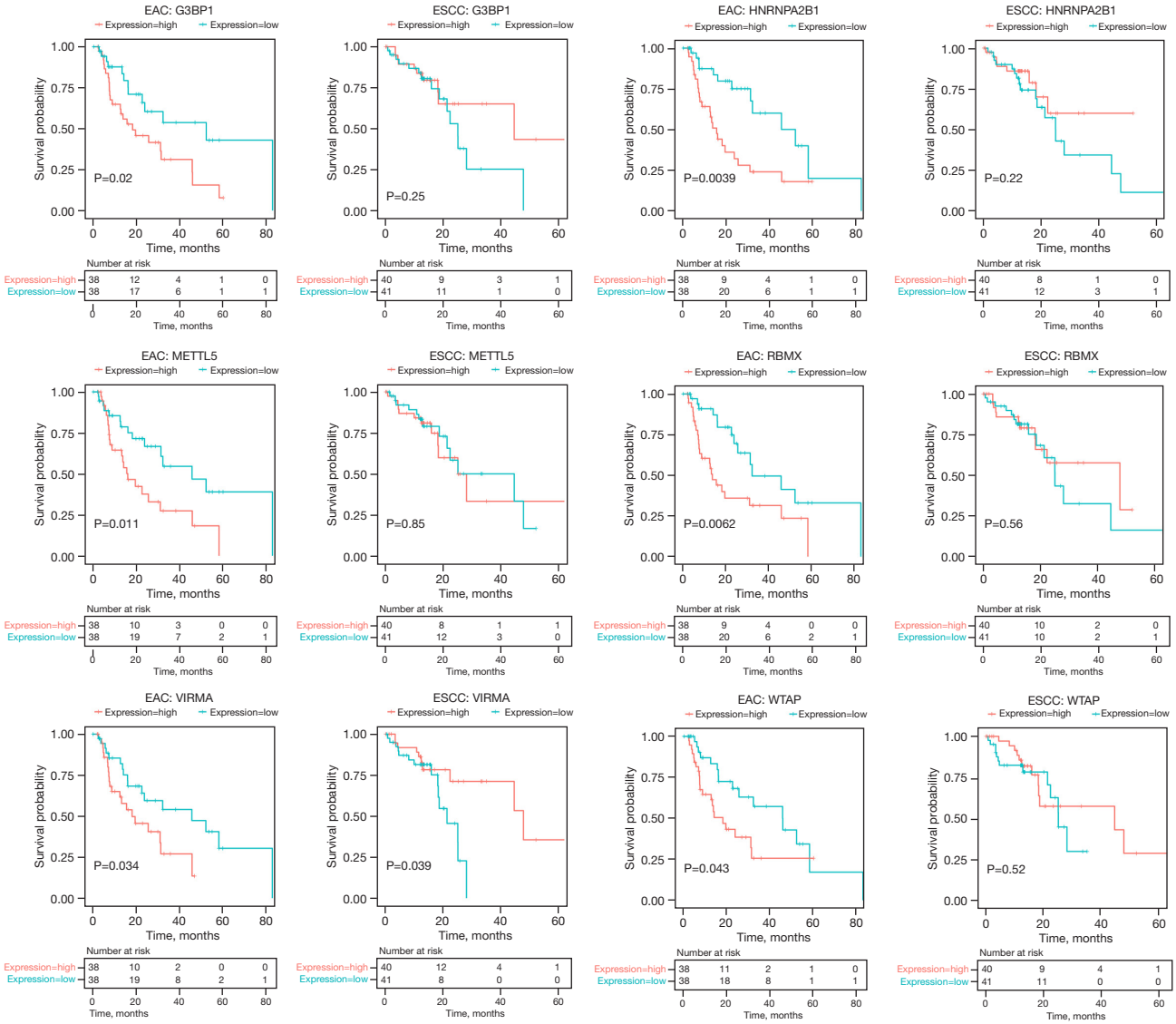

Figure 2 The relationship between m6A regulator expression and the overall survival of patients, evaluated based on the TCGA-ESCA transcriptome data. m6A, N6-methyladenosine; TCGA, The Cancer Genome Atlas; ESCA, esophageal cancer.

examined (*Figure 5*). In EAC, *YTHDC2* was most closely related to activating cancer pathways, including protein secretion, *PI3K/AKT/MTOR* signaling, *p53* pathway, UV response, and heme metabolism. In ESCC, *ALKBH5* was mostly associated with the activation of cancer pathways, including *Wnt/beta/catenin* signaling, mitotic spindle, unfolded protein response, heme metabolism, and glycolysis.

In addition, the expression of most m6A regulators was positively correlated with cancer-associated pathways in EAC and negatively correlated with cancer-associated pathways in ESCC. To further examine the opposing role of *VIRMA* in ESCC and EAC prognosis, *in vivo* and *in vitro* functional assays were performed. *VIRMA* was positively correlated with the activation of the myogenesis and *KRAS* signaling pathways in EAC, but negatively correlated with the pathways in ESCC.

m6A regulators are usually involved in biological processes in the form of cooperation between methylation/demethylases and RNA-binding proteins. For tumor-associated mRNA, m6A readers regulate the expression levels of target proteins by affecting RNA degradation

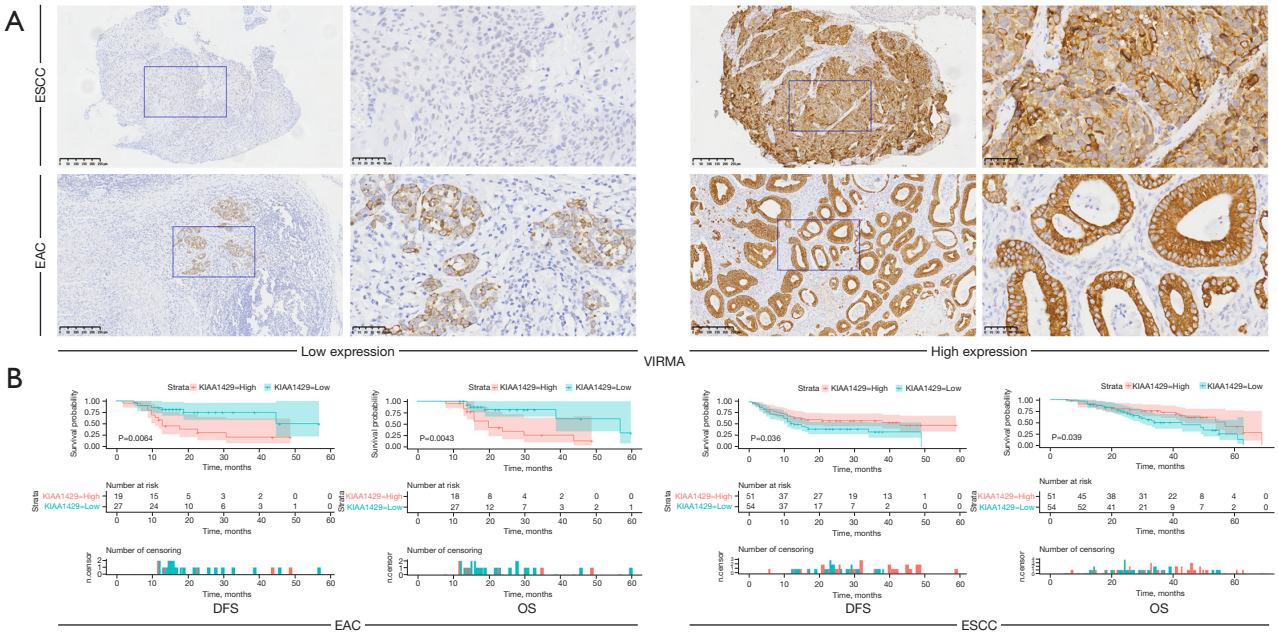

Figure 3 The relationship between *VIRMA* protein expression levels and survival, based on a single-center validation cohort. (A) Representative immunohistochemistry images of low and high *VIRMA* expression (×200 and ×400 magnification). (B) The relationship between *VIRMA* protein expression levels and survival. ESCC, esophageal squamous cell carcinoma; EAC esophageal adenocarcinoma; DFS, disease-free survival (the time interval from the surgery to disease progression); OS, overall survival (the time from the surgery to the patient's death).

and translation after methylation/demethylation. For example, *YTHDF1* regulates lipid metabolism and affects the progression of esophageal cancer by reducing the translation efficiency of m6A modified *HSD17B11* mRNA (15). In terms of non-coding RNA, m6a-related genes silence or inhibit the expression of target genes by affecting transcription, splicing, and translation. For example, *HNRNPA2B1* promotes the proliferation of ESCC cells by binding a m6A-modified *miR-17-92* cluster and upregulating the expression of *miR-17-92* cluster (16). Therefore, we analyzed the correlation rate of m6A regulators in EAC and ESCC separately. The m6A regulator correlation rate was higher in EAC than in ESCC (*Figure 6A*). Analysis of the top five groups with the highest correlation rate between writers and readers in EAC revealed that four of them had a lower correlation in ESCC (*Figure 6A,6B*). This suggested that the synergistic effect of writers and readers in m6A regulators in EAC is superior to that in ESCC, and this may lead to the expression of m6A regulators in EAC that can promote tumor development.

The relationship between immune checkpoint proteins and m6A regulators was analyzed. The overall correlation between m6A regulators and immune checkpoint proteins was weaker in EC (*Figure 6C,6D*). The tumor purity score and proportion of immune cell infiltration were calculated using the R packages ESTIMATE and MCP-counter, respectively, and the correlation between m6A methylation regulators was analyzed (*Figure 6E,6F*). We found that there were more negative correlations between eraser and reader with stromal and immune cell scores in ESCC than in EAC, suggesting that the occurrence of demethylation in ESCC may be related to immune-desert phenotype. From the data, *FTO* in EAC, as well as *METTL5* and *WTAP* in ESCC were found to be highly correlated with the immune matrix score. These correlations may be useful in predicting tumor efficacy and the development of effective intervention targets.

Association of m6A regulators with immunotherapy sensitivity in EC

The GSE165252 dataset was downloaded from the GEO, and the samples were divided into a sensitive group (responder) and a drug-resistant group (non-responder)

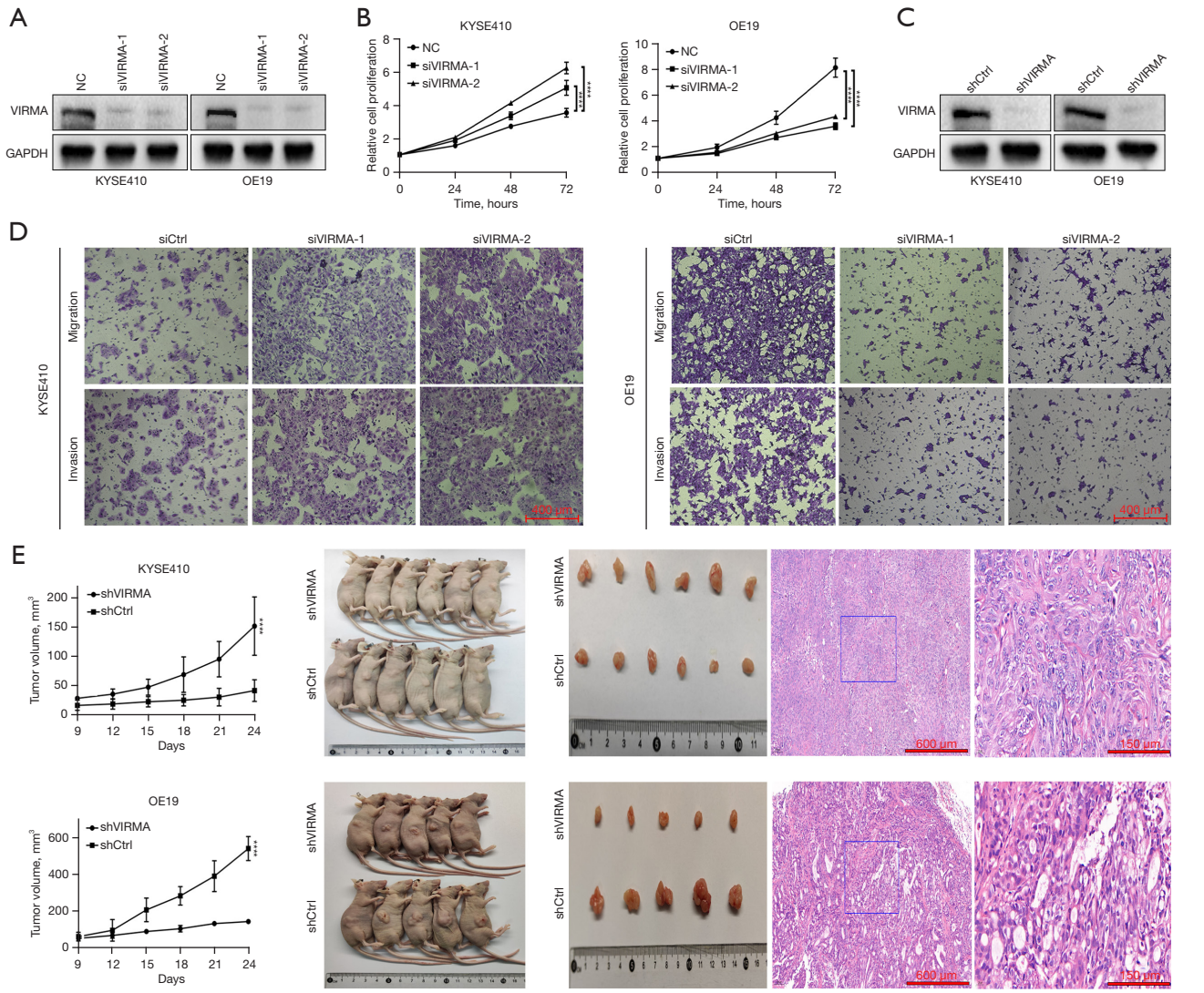

Figure 4 *In vivo* and *in vitro* functional assay involving *VIRMA*. (A) Western blot analysis of *VIRMA* expression efficiency in siRNA knockdown KYSE410 and OE19 cells. (B) The CCK-8 assay was used to detect the viability of KYSE410 and OE19 cells transfected with *VIRMA* siRNAs or control. (C) Western blot analysis of *VIRMA* expression efficiency in shRNA knockdown KYSE410 and OE19 cells. (D) The Transwell assay was performed to detect the migration and invasion ability of KYSE410 and OE19 cells transfected with *VIRMA* siRNAs or control. Stained with 3% crystal violet in methanol. (E) Subcutaneous tumorigenicity assay of KYSE410 and OE19 cells transfected with *VIRMA* shRNA or control, the right side is the H&E staining of the tumor. Data are representative of at least three independent experiments. Data are presented as mean ± SEM. ****, P<0.0001. NC, negative control; H&E, hematoxylin and eosin; SEM, standard error of the mean.

according to the provided clinical data. The results showed that all m6A methylation regulators were included in the EAC immunotherapy data. There was no significant difference in the expression levels between the centrally sensitive and resistant groups (*Figure 6G*; P values were all greater than 0.05).

Currently, there are no public ESCC immunotherapy-related databases available. We retrospectively collected data from 40 patients with ESCC from our hospital who received concurrent immunotherapy and radiotherapy followed by surgical resection. The relationship between immunotherapy sensitivity and m6A regulator expression levels was assessed by IHC of pre-treatment biopsy specimens. Due to the limited number of biopsy specimens,

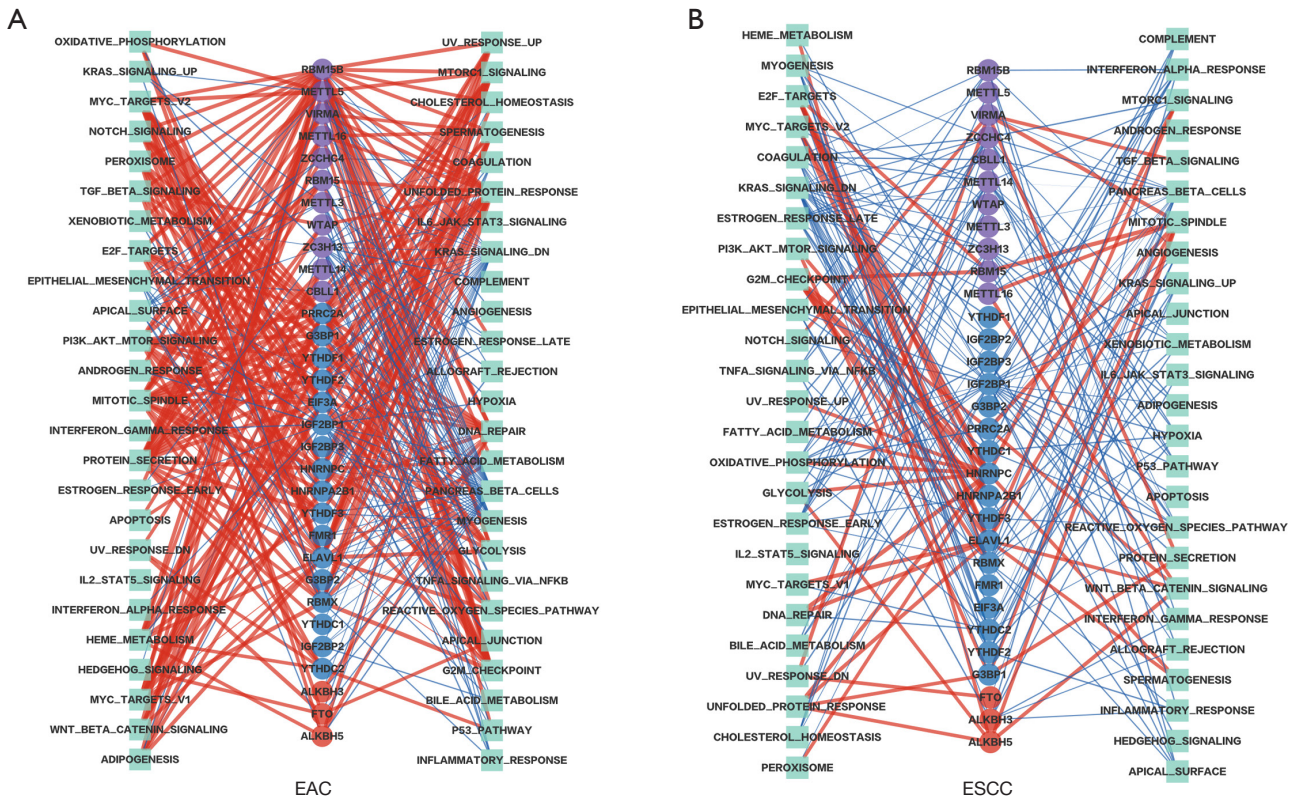

Figure 5 The network diagram displays the relationship between the selected m6A regulators and cancer hallmark-related pathways in (A) EAC and (B) ESCC from the TCGA-ESCA cohort. The red and blue lines represent positive and negative correlations, respectively. EAC, esophageal adenocarcinoma; ESCC, esophageal squamous cell carcinoma; TCGA, The Cancer Genome Atlas; ESCA, esophageal cancer.

we selected five metrics (*WTAP*, *VIRMA*, *RBM15B*, *FTO*, and *METTL14*) related to the tumor purity score and immune cell infiltration, as shown in *Figure* 7. The expression level of the *FTO* protein was significantly correlated with the sensitivity of ESCC to immunotherapy combined with radiotherapy, and patients with low *FTO* expression were more sensitive (*Table 2*).

Discussion

As the most important internal epigenetic modification of mRNAs in eukaryotes, the level of m6A affects RNA processing, degradation, translation, gene expression, and key cellular processes, ultimately affecting the occurrence and development of tumors and therapeutic efficacy (17). In this study, we focused on the two major pathological types of EC, SCC and AC. We analyzed the expression patterns and genetic variation of m6A regulators, as well as their associations with clinicopathological factors, prognosis, tumor pathways, and immune signatures in ESCC and EAC.

The study demonstrated that m6A regulators differed significantly in their expression patterns and genetic variation between ESCC and EAC. Differentially expressed regulators were significantly elevated in ESCC compared to EAC. There were also significant differences between the two groups in terms of methylation levels, CNVs, and somatic mutations. This is consistent with the large differences between ESCC and EAC reported in previous studies (4,18). To our knowledge, this is the first study to provide comprehensive data on the differences between ESCC and EAC in terms of m6A regulators.

In different pathological types, m6A regulators play different roles. *METTL3* can promote the progression of leukemia (19), colorectal cancer (20), and prostate cancer (21), but prolong the survival of glioblastoma (22). Overexpression of *ALKBH5* is associated with tumor progression in ovarian cancer (23) and gastric cancer (24), but it acts as a tumor

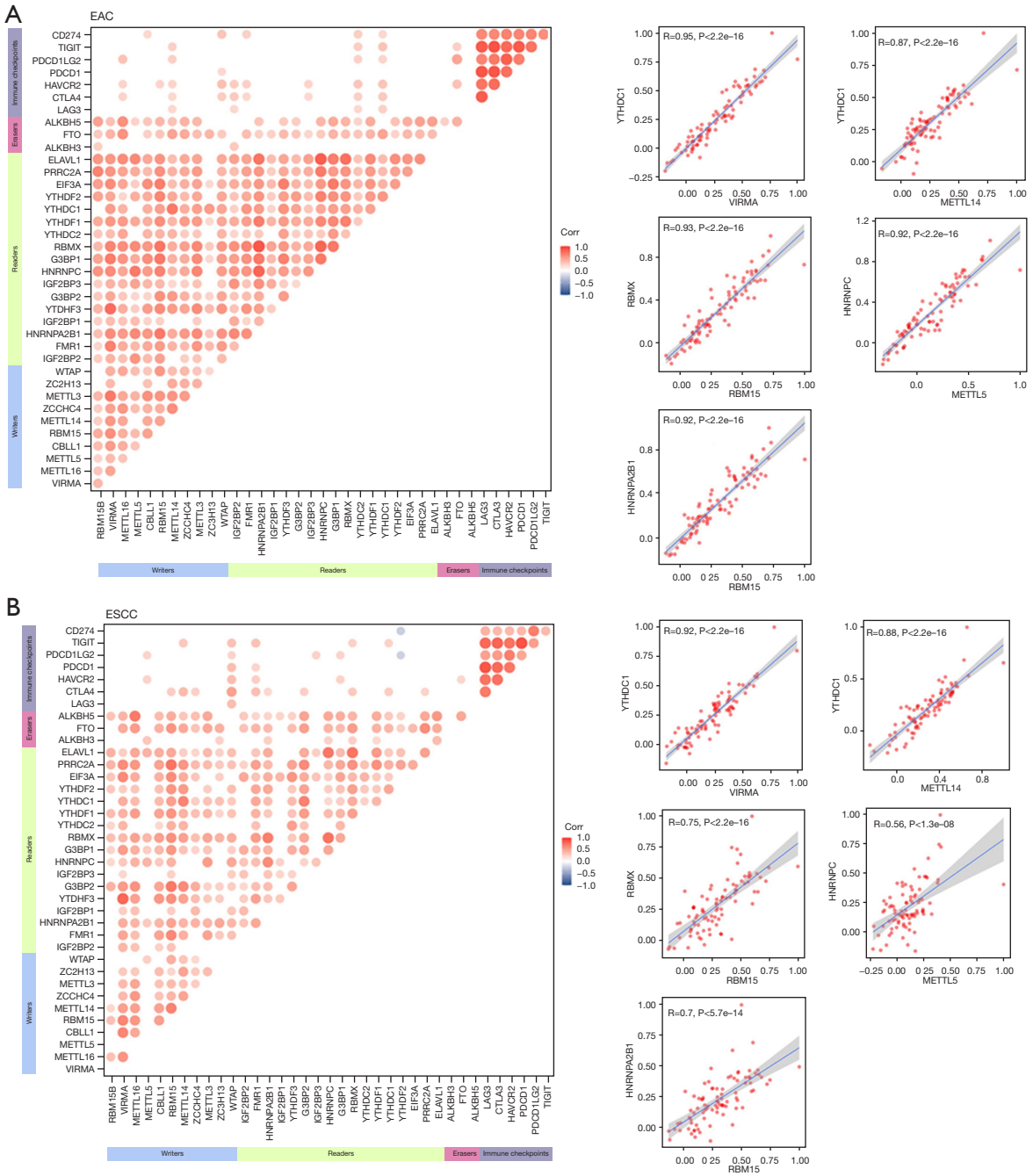

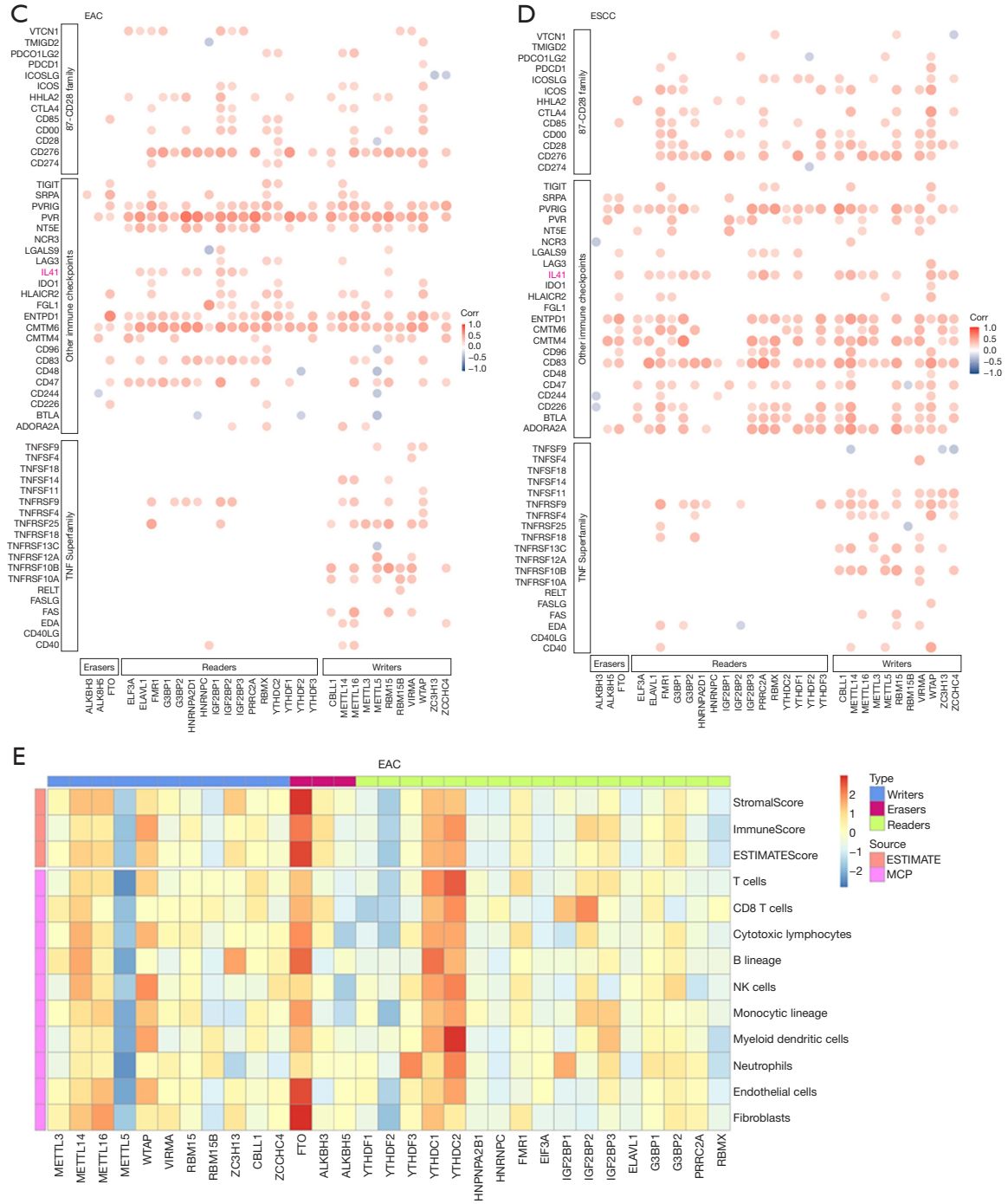

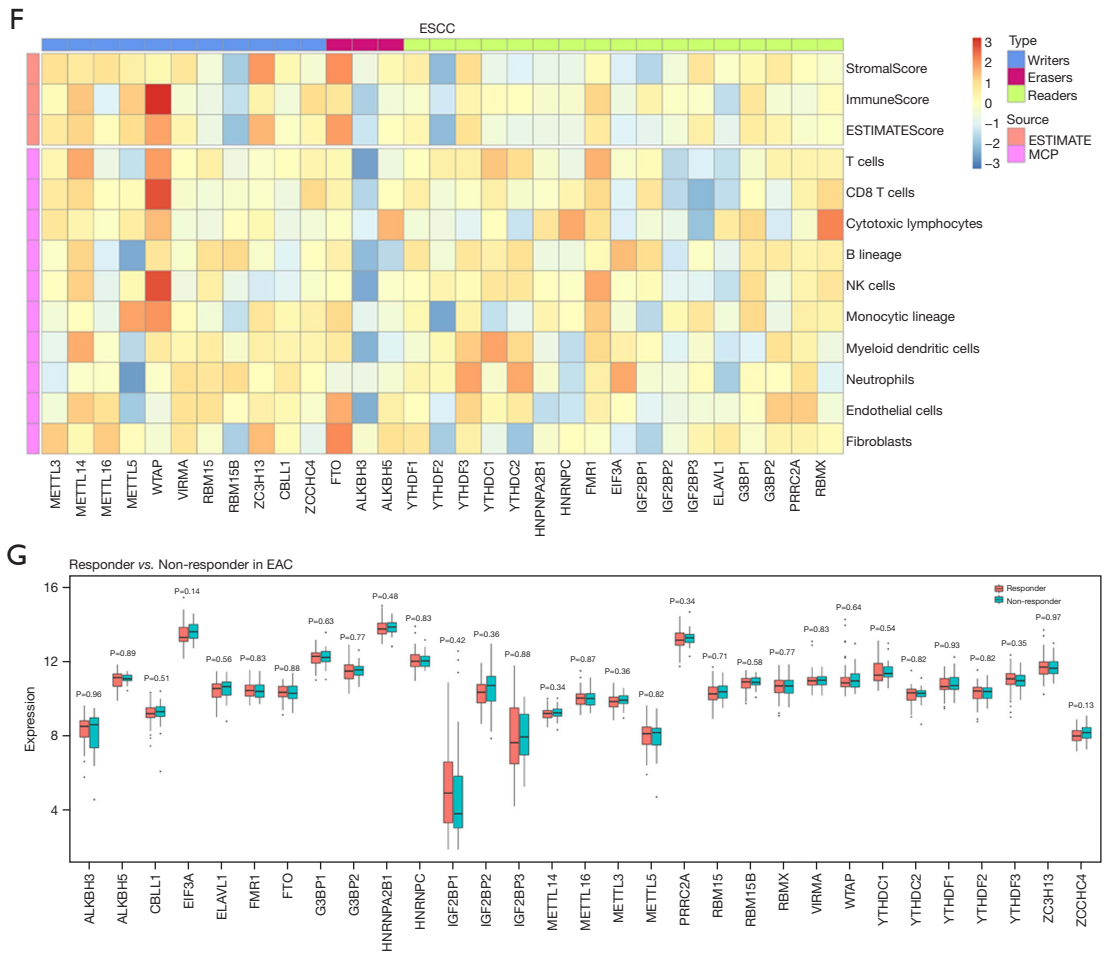

Figure 6 The association between m6A regulators with immune characteristics. (A,B) The correlations between m6A regulators in the TCGA-ESCA transcriptome data and the top five groups of writers and readers with the highest correlations. (C,D) Heatmaps showing the correlations between 60 immune checkpoint proteins and m6A regulators in EAC and ESCC. (E,F) Heatmaps of the correlation between m6A regulator expression and the tumor purity score and immune cell infiltration ratio. (G) An analysis of the relationship between m6A regulator expressions and EAC immunotherapy sensitivity based on the GSE165252 dataset. Red represents the sensitive group (responder) and green represents the drug-resistant group (non-responder). EAC esophageal adenocarcinoma; ESCC, esophageal squamous cell carcinoma; m6A, N6-methyladenosine; TCGA, The Cancer Genome Atlas; ESCA, esophageal cancer.

suppressor gene in pancreatic cancer (25).

Analysis of public databases revealed a significant correlation between m6A modulators and EC tumor stage and prognosis. *VIRMA* expression levels showed a reverse correlation with prognosis in ESCC and EAC. Retrospective analysis of 105 ESCC and 46 EAC patients from our hospital revealed that ESCC patients with high *VIRMA* expression had good prognosis, and conversely, EAC patients with high *VIRMA* expression had poor prognosis. To further explore the functional differences in *VIRMA* between ESCC and EAC, we knocked down *VIRMA* expression in ESCC and EAC cell lines. *In vivo* and *in vitro* functional experiments showed that the proliferation, invasion, migration, and tumorigenic abilities of ESCC and EAC cells were significantly altered after *VIRMA* knockdown, and the two cell lines showed opposite trends. Previous publications have shown that breast cancer (26) and hepatocellular carcinoma (13) with high *VIRMA* expression had a prognosis, while renal clear cell carcinoma (27), renal papillary cell carcinoma (28), and papillary thyroid carcinoma (29) showed good prognosis. Gastric ACs and EACs are closely related. A study has

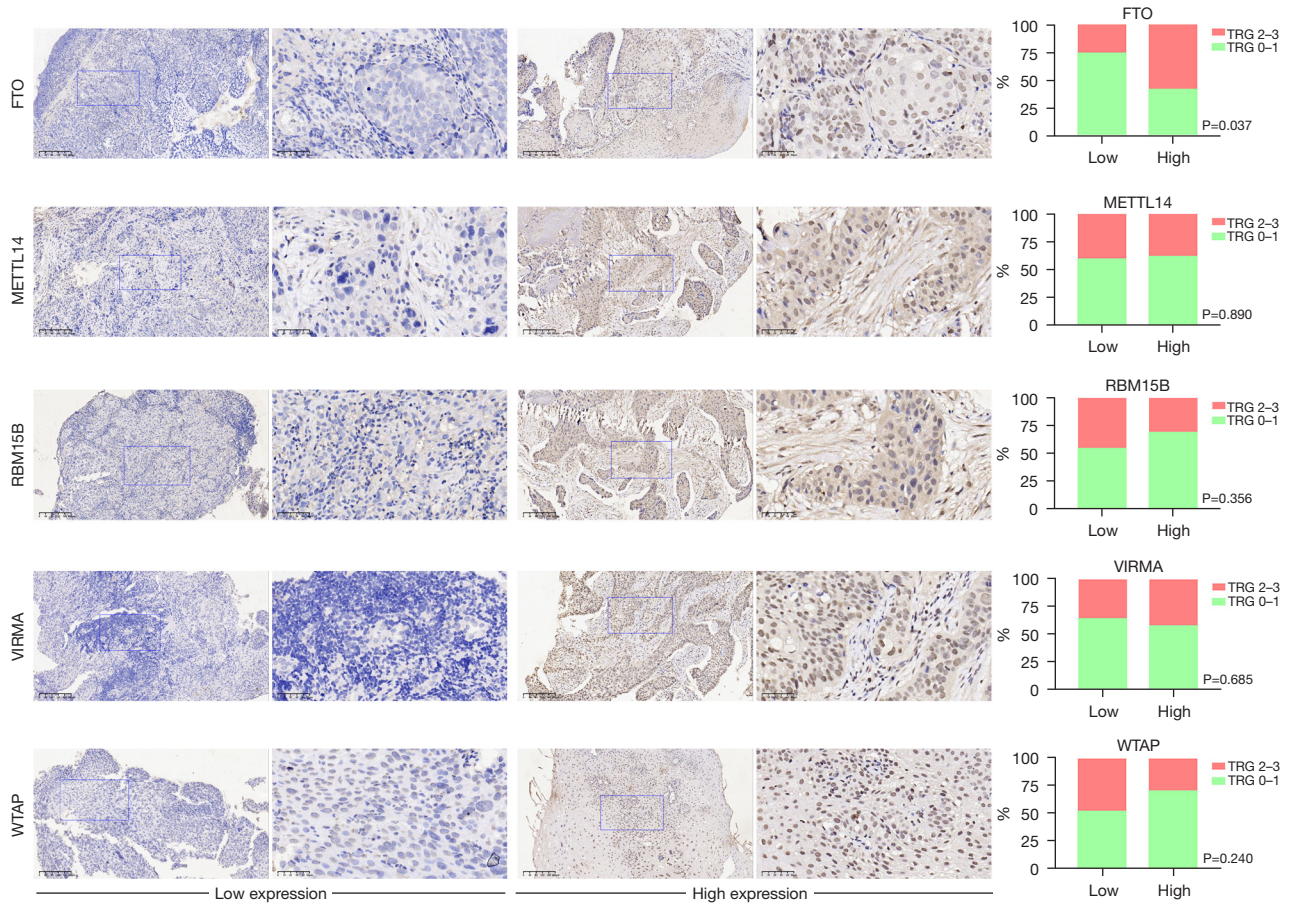

Figure 7 The relationship between IHC expression of five m6A regulators and tumor regression grade in a neoadjuvant immunotherapy validation cohort for ESCC. (Left) Representative images of high and low expression in immunohistochemistry (×200 and ×400 magnification). (Right) Stacked histogram of tumor regression grade versus m6A regulator IHC score for patients in the neoadjuvant immunotherapy validation cohort. The X-axis is the high expression and low expression of IHC, and the Y-axis is the percentage of each type of patient. The data in the figure are from *Table 1*. m6A, N6-methyladenosine; ESCC, esophageal squamous cell carcinoma; IHC, immunohistochemistry.

demonstrated that gastric AC with high *VIRMA* levels are associated with late stage and poor prognosis, and *VIRMA* promoted the progression of gastric AC (30). This supports the opposing prognostic effects of VIMRA in ESCC and EAC observed in our study.

Expression of m6A regulators was positively correlated with various cancer-related pathways in EAC, and mostly negatively correlated with cancer pathways in ESCC. Our findings also illustrated the significant differences between EAC and ESCC in terms of tumorigenesis and development pathways.

M6A plays an important role in the tumor immune microenvironment, which in turn affects the occurrence, development and treatment sensitivity of tumors. A study has shown that key functions in regulatory T cells have a clear m6A mRNA dependence, making them potentially important targets in anti-tumor immunotherapy (31). The methylase *METTL14* plays an important role in the development of B cells, and its downregulation can lead to severe developmental defects in all B cells (32). The methylase *METTL3* can mediate the activation and function of dendritic cells (33). Silencing of the demethylase *FTO* significantly inhibits the polarization of M1 and M2 macrophages (34). Elevated *METTL3* levels in $CD33^{+}$ myeloid-derived suppressor cells (MDSCs) are associated with poor prognosis (35), and knockdown of *METTL3* attenuates tumor-associated MDSC differentiation (36). M6a is closely related to the expression of PD-L1. In colon cancer

Table 2 Clinical characteristics and IHC expressions of the ESCC immunotherapy validation cohort

Variables	TRG0-1	TRG2-3	P value
Sex			0.601
Male	18	13	
Female	6	3	
Age (years)			0.938
≤60	11	6	
>60	13	10	
TNM stage			0.515
II	8	16	
III	3	13	
VIRMA			0.685
Low	9	5	
High	15	11	
RBM15B			0.356
Low	13	11	
High	11	5	
FTO			0.037
Low	17	6	
High	7	10	
METTL14			0.890
Low	16	11	
High	8	5	
WTAP			0.240
Low	12	11	
High	12	5	

Tumor staging was performed according to the NCCN Esophageal and Esophagogastric Junction Cancers Guidelines Version 3.2022. High and low represent the protein expression of IHC. IHC, immunohistochemistry; ESCC, esophageal squamous cell carcinoma; NCCN, National Comprehensive Cancer Network; TNM, Primary Tumor Regional Lymph Nodes Distant Metastasis.

cells, the demethylase *FTO* can regulate the methylation of PD-L1, thereby affecting its expression level (37). In ESCC, the expression of PD-L1 was significantly negatively correlated with the expression levels of *YTHDF2*, *METL14*, and *KIAA1429* (38). M6A regulators in EC correlate with levels of immune cell infiltration (39). *YTHDC2* is associated with the level of immune infiltration of B cells, $CD8^+$ T cells, $CD4^+$ T cells, neutrophils and dendritic cells in head and neck squamous cell carcinoma (40). We analyzed the relationships between m6A expression levels and immune checkpoint proteins, the tumor purity score, and immune cell infiltration ratio in both ESCC and EAC. To study the efficacy of immune checkpoint inhibitors, we selected patients who received neoadjuvant radiotherapy combined with immunotherapy. It is more convincing to use surgical pathology after neoadjuvant therapy to evaluate the degree of tumor regression and sensitivity. The m6A regulators could not distinguish between responders and non-responders in the EAC. The demethylase *FTO* was significantly associated with the efficacy of immunotherapy in patients with ESCC, and patients with low *FTO* expression were more sensitive. This is consistent with previous study showing that targeting *FTO* has good therapeutic effects, including inhibiting tumor growth, enhancing immunotherapy, and reducing drug resistance (41). In the EAC group, no potential predictors were identified, and this may be related to the limitations of the transcriptome data and the small number of samples.

This investigation examined the role of m6A regulators in ESCC and EAC from multiple aspects, such as tumor occurrence and development, immunotherapy sensitivity, and prognosis. Data from online databases were analyzed and the findings were verified using clinical samples, as well as *in vivo* and *in vitro* experiments. There were some limitations to this study, such as the lack of a multicenter validation cohort and the absence of prospective validation. Nonetheless, this report provides a molecular basis to elucidate the similarities and differences between ESCC and EAC, and suggests that m6A regulators may be effective targets for improving ESCC and EAC treatment.

Conclusions

M6A regulators play an important role in the development, treatment sensitivity and prognosis of ESCC and EAC, respectively. *VIRMA* and *FTO* may be potential intervention targets for ESCC.

Acknowledgments

Funding: This work was funded by the National Natural Science Foundation of China (No. 81874224), the Academic Promotion Program of Shandong First Medical University (No. 2019LJ004), the Taishan Scholar Construction Project

(No. ts20120505), and the Tumor Prevention and Control Joint Fund of Shandong Province Natural Science Fund, China (No. ZR2019LZL008).

Footnote

Reporting Checklist: The authors have completed the ARRIVE reporting checklist. Available at https://atm.amegroups.com/article/view/10.21037/atm-22-5895/rc

Data Sharing Statement: Available at https://atm.amegroups.com/article/view/10.21037/atm-22-5895/dss

Conflicts of Interest: All authors have completed the ICMJE uniform disclosure form (available at https://atm.amegroups.com/article/view/10.21037/atm-22-5895/coif). The authors have no conflicts of interest to declare.

Ethical Statement: The authors are accountable for all aspects of the work in ensuring that questions related to the accuracy or integrity of any part of the work are appropriately investigated and resolved. The study was conducted in accordance with the Declaration of Helsinki (as revised in 2013). The use of the validation cohort in this study was approved by the Ethics Committee of Shandong Cancer Hospital (approval No. SDTHEC201803). Since the validation cohort was retrospective in nature, the requirement for informed consent was waived. Animal experiments were performed under a project license (No. SDTHEC201803) granted by the Ethics Committee of Shandong Cancer Hospital, in compliance with institutional guidelines for the care and use of animals.

References

1. Bray F, Ferlay J, Soerjomataram I, et al. Global cancer statistics 2018: GLOBOCAN estimates of incidence and mortality worldwide for 36 cancers in 185 countries. CA Cancer J Clin 2018;68:394-424.
2. Siegel RL, Miller KD, Jemal A. Cancer statistics, 2020. CA Cancer J Clin 2020;70:7-30.
3. Sun JM, Shen L, Shah MA, et al. Pembrolizumab plus chemotherapy versus chemotherapy alone for first-line treatment of advanced oesophageal cancer (KEYNOTE-590): a randomised, placebo-controlled, phase 3 study. Lancet 2021;398:759-71.
4. Zhang X, Wang Y, Meng L. Comparative genomic analysis of esophageal squamous cell carcinoma and adenocarcinoma: New opportunities towards molecularly targeted therapy. Acta Pharm Sin B 2022;12:1054-67.
5. Schiffmann LM, Plum PS, Fuchs HF, et al. Tumor Microenvironment of Esophageal Cancer. Cancers (Basel) 2021;13:4678.
6. Nombela P, Miguel-López B, Blanco S. The role of m(6)A, m(5)C and Ψ RNA modifications in cancer: Novel therapeutic opportunities. Mol Cancer 2021;20:18.
7. Li Y, Xiao J, Bai J, et al. Molecular characterization and clinical relevance of m(6)A regulators across 33 cancer types. Mol Cancer 2019;18:137.
8. Liu J, Harada BT, He C. Regulation of Gene Expression by N(6)-methyladenosine in Cancer. Trends Cell Biol 2019;29:487-99.
9. Huang H, Weng H, Chen J. m(6)A Modification in Coding and Non-coding RNAs: Roles and Therapeutic Implications in Cancer. Cancer Cell 2020;37:270-88.
10. Tian J, Wei X, Zhang W, et al. Effects of Selenium Nanoparticles Combined With Radiotherapy on Lung Cancer Cells. Front Bioeng Biotechnol 2020;8:598997.
11. Shen Z, Gu L, Liu Y, et al. PLAA suppresses ovarian cancer metastasis via METTL3-mediated m(6)A modification of TRPC3 mRNA. Oncogene 2022;41:4145-58.
12. Yu H, Yang X, Tang J, et al. ALKBH5 Inhibited Cell Proliferation and Sensitized Bladder Cancer Cells to Cisplatin by m6A-CK2α-Mediated Glycolysis. Mol Ther Nucleic Acids 2021;23:27-41.
13. Lan T, Li H, Zhang D, et al. KIAA1429 contributes to liver cancer progression through N6-methyladenosine-dependent post-transcriptional modification of GATA3. Mol Cancer 2019;18:186.
14. Wang T, Kong S, Tao M, et al. The potential role of RNA N6-methyladenosine in Cancer progression. Mol Cancer 2020;19:88.

15. Duan X, Yang L, Wang L, et al. m6A demethylase FTO promotes tumor progression via regulation of lipid metabolism in esophageal cancer. Cell Biosci 2022;12:60.
16. Li K, Chen J, Lou X, et al. HNRNPA2B1 Affects the Prognosis of Esophageal Cancer by Regulating the miR-17-92 Cluster. Front Cell Dev Biol 2021;9:658642.
17. Zhou Z, Lv J, Yu H, et al. Mechanism of RNA modification N6-methyladenosine in human cancer. Mol Cancer 2020;19:104.
18. Wu H, Yu J, Li Y, et al. Single-cell RNA sequencing reveals diverse intratumoral heterogeneities and gene signatures of two types of esophageal cancers. Cancer Lett 2018;438:133-43.
19. Vu LP, Pickering BF, Cheng Y, et al. The N(6)-methyladenosine (m(6)A)-forming enzyme METTL3 controls myeloid differentiation of normal hematopoietic and leukemia cells. Nat Med 2017;23:1369-76.
20. Peng W, Li J, Chen R, et al. Upregulated METTL3 promotes metastasis of colorectal Cancer via miR-1246/SPRED2/MAPK signaling pathway. J Exp Clin Cancer Res 2019;38:393.
21. Li E, Wei B, Wang X, et al. METTL3 enhances cell adhesion through stabilizing integrin β1 mRNA via an m6A-HuR-dependent mechanism in prostatic carcinoma. Am J Cancer Res 2020;10:1012-25.
22. Visvanathan A, Patil V, Arora A, et al. Essential role of METTL3-mediated m(6)A modification in glioma stem-like cells maintenance and radioresistance. Oncogene 2018;37:522-33.
23. Zhu H, Gan X, Jiang X, et al. ALKBH5 inhibited autophagy of epithelial ovarian cancer through miR-7 and BCL-2. J Exp Clin Cancer Res 2019;38:163.
24. Zhang J, Guo S, Piao HY, et al. ALKBH5 promotes invasion and metastasis of gastric cancer by decreasing methylation of the lncRNA NEAT1. J Physiol Biochem 2019;75:379-89.
25. Tang B, Yang Y, Kang M, et al. m6A demethylase ALKBH5 inhibits pancreatic cancer tumorigenesis by decreasing WIF-1 RNA methylation and mediating Wnt signaling. Mol Cancer 2020;19:3.
26. Qian JY, Gao J, Sun X, et al. KIAA1429 acts as an oncogenic factor in breast cancer by regulating CDK1 in an N6-methyladenosine-independent manner. Oncogene 2019;38:6123-41.
27. Lobo J, Barros-Silva D, Henrique R, et al. The Emerging Role of Epitranscriptomics in Cancer: Focus on Urological Tumors. Genes (Basel) 2018.
28. Sun Z, Jing C, Xiao C, et al. Prognostic risk signature based on the expression of three m6A RNA methylation regulatory genes in kidney renal papillary cell carcinoma. Aging (Albany NY) 2020;12:22078-94.
29. Hou J, Shan H, Zhang Y, et al. m(6)A RNA methylation regulators have prognostic value in papillary thyroid carcinoma. Am J Otolaryngol 2020;41:102547.
30. Miao R, Dai CC, Mei L, et al. KIAA1429 regulates cell proliferation by targeting c-Jun messenger RNA directly in gastric cancer. J Cell Physiol 2020;235:7420-32.
31. Chen M, Wei L, Law CT, et al. RNA N6-methyladenosine methyltransferase-like 3 promotes liver cancer progression through YTHDF2-dependent posttranscriptional silencing of SOCS2. Hepatology 2018;67:2254-70.
32. Li M, Zha X, Wang S. The role of N6-methyladenosine mRNA in the tumor microenvironment. Biochim Biophys Acta Rev Cancer 2021;1875:188522.
33. Wang H, Hu X, Huang M, et al. Mettl3-mediated mRNA m(6)A methylation promotes dendritic cell activation. Nat Commun 2019;10:1898.
34. Gu X, Zhang Y, Li D, et al. N6-methyladenosine demethylase FTO promotes M1 and M2 macrophage activation. Cell Signal 2020;69:109553.
35. Shang W, Gao Y, Tang Z, et al. The Pseudogene Olfr29-ps1 Promotes the Suppressive Function and Differentiation of Monocytic MDSCs. Cancer Immunol Res 2019;7:813-27.
36. Ni HH, Zhang L, Huang H, et al. Connecting METTL3 and intratumoural CD33(+) MDSCs in predicting clinical outcome in cervical cancer. J Transl Med 2020;18:393.
37. Tsuruta N, Tsuchihashi K, Ohmura H, et al. RNA N6-methyladenosine demethylase FTO regulates PD-L1 expression in colon cancer cells. Biochem Biophys Res Commun 2020;530:235-9.
38. Guo W, Tan F, Huai Q, et al. Comprehensive Analysis of PD-L1 Expression, Immune Infiltrates, and m6A RNA Methylation Regulators in Esophageal Squamous Cell Carcinoma. Front Immunol 2021;12:669750.
39. Zhao H, Xu Y, Xie Y, et al. m6A Regulators Is Differently Expressed and Correlated With Immune Response of Esophageal Cancer. Front Cell Dev Biol 2021;9:650023.
40. Li Y, Zheng JN, Wang EH, et al. The m6A reader protein

YTHDC2 is a potential biomarker and associated with immune infiltration in head and neck squamous cell carcinoma. PeerJ 2020;8:e10385.

41. Li Y, Su R, Deng X, et al. FTO in cancer: functions, molecular mechanisms, and therapeutic implications. Trends Cancer 2022;8:598-614.

Cite this article as: Li Z, Zheng C, Huang L, Yin X, Wang Z, Liu C, Li B. The landscape of m6A regulators in esophageal cancer: molecular characteristics, immuno-oncology features, and clinical relevance. Ann Transl Med 2022;10(24):1347. doi: 10.21037/atm-22-5895

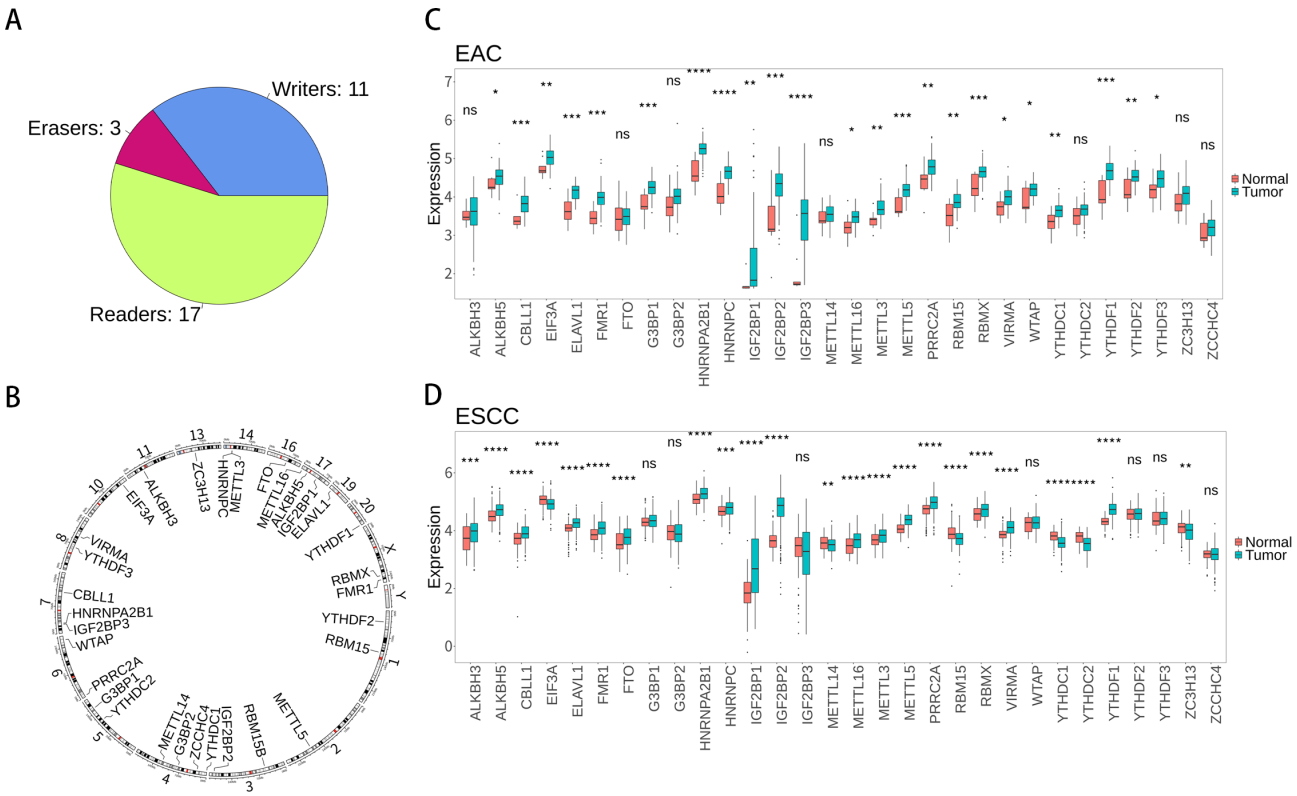

Figure S1 (A) Classification of the 31 m6A regulators. (B) Genome distribution of the 31 m6A regulators. (C) A comparison of the m6A regulators expression levels in EAC tumors and normal tissues in the TCGA-ESCA dataset. Red represents normal samples and green represents tumor samples. (D) A comparison of the expression levels in ESCC tumors and normal tissues in the TCGA-ESCA and GSE53625 datasets. Red represents normal samples and green represents tumor samples. NS, no significant. *, P<0.05, **, P<0.01, ***, P<0.001, ****, P<0.0001.

https://dx.doi.org/10.21037/atm-22-5895

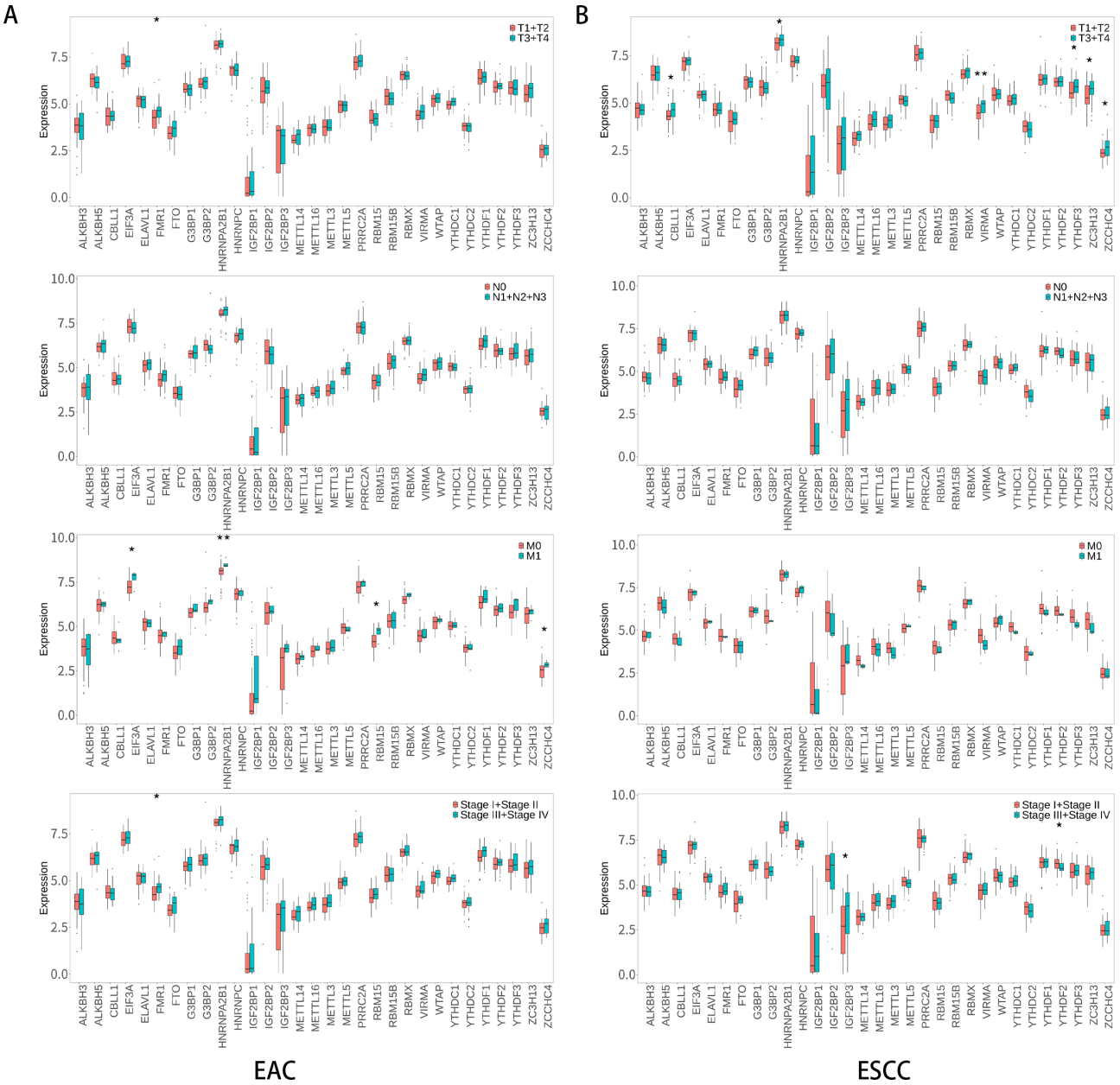

Figure S2 The association between m6A regulators and tumor stage in (A) EAC and (B) ESCC samples from the TCGA-ESCC cohort. The analysis was performed with four aspects: primary tumor (T stage), regional lymph nodes (N stage), distant metastasis (M stage), and clinical staging. *, P<0.05, **, P<0.01.

https://dx.doi.org/10.21037/atm-22-5895